

**DYNAMIC FIELD PLOTS OF SINGLE AND COUPLED
MICROSTRIP LINES[†]**

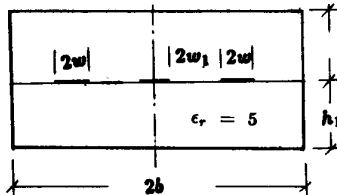
Ayman A. Mostafa ^{*}, Clifford M. Krowne [†], and Kawthar A. Zaki ^{*}

^{*} University of Maryland, Dept. of Electrical Eng., College Park, MD 20742.

[†] Code 6851, Elec. Tech. Division, NRL, Washington, D.C. 20375-5000.

Introduction

The propagation constant γ of guided wave structures is much more accurately found numerically than the electric and magnetic fields. Most of the line properties can be ascertained from γ and the characteristic impedance Z . However, little effort has been expended previously on generating 2D field plots for dispersive planar integrated circuits. In this paper dynamic field plots are provided for single and coupled strip structures over isotropic dielectric layers.



Analysis

The propagation modes on planar transmission line are assumed to be hybrid which are superposition of TE and TM fields derivable from two independent potential functions. The finite fourier transform is defined as

$$\tilde{\phi}(\alpha_n, y) = \int_{-b}^b \phi(x, y) e^{-j\alpha_n x} dx \quad (1)$$

Where tilde $\tilde{}$ denotes the fourier transform and $\alpha_n = (2n+1)\pi/2b$ or $n\pi/b$ for even and odd modes respectively. The inverse fourier transform is

$$\phi(x, y) = 1/2b \sum_{n=-\infty}^{\infty} \tilde{\phi}(\alpha_n, y) e^{j\alpha_n x} \quad (2)$$

Expressing the fields ($\tilde{E}_x, \tilde{E}_y, \tilde{E}_z, \tilde{H}_x, \tilde{H}_y, \tilde{H}_z$) in terms of the potential functions and matching the boundary conditions, one gets the dispersion equation for β [1]. By solving this equation, the strip currents are found and hence the fields are determined.

[†] Work supported in part by NRL Contract No. N0014-86-K-2013.

The electric and magnetic lines are solutions of the first order differential equation [2,3]

$$\frac{dy}{dx} = \frac{E_y(x,y)}{E_x(x,y)} \quad (3)$$

Discretizing this equation leads to

$$x_{i+1} = x_i + \delta x_i \quad ; \quad y_{i+1} = y_i + \delta y_i \quad (4a)$$

$$\delta x_i = \frac{E_x}{\sqrt{E_x^2 + E_y^2}} \quad ; \quad \delta y_i = \frac{E_y}{\sqrt{E_x^2 + E_y^2}} \quad (4b)$$

Where (x_i, y_i) is the present field point and (x_{i+1}, y_{i+1}) is the next point.

Equation (2) is used at each point (x,y) along the line of force to calculate the fields back in the space domain. The series (2) converges wherever the fields are finite. To minimize the CPU time required for the calculation of the inverse fourier transform, the following observations have been taken into account:

(1) The convergence of the series is different from point to point.

(2) The rate of convergence of the series (2) is almost independent of x for a given y , but is a very fast varying function of y for a given x . Along the dielectric interface ($y = h_1$), the series has the asymptote $e^{j\alpha_n(x-w)} / \sqrt{n}$ for large n . Such a series is a conditionally and a very slowly convergent one (it diverges at the strip edge $x = w$ for some field components).

To speed up the convergence of the slow series at the interface $y = h_1$, the Mellin transform is used [4]. For example for a single strip line, the dominant mode E_y is even with respect to x and it is expressed as

$$E_y(x) = 1/b \sum_{n=0}^{\infty} \tilde{E}_y(n) \cos(\alpha_n x) \quad (5)$$

Using the Mellin transform [4], E_y can be expressed as

$$E_y(x) = 1/b \left[\sum_{n=0}^N \tilde{E}_y(n) \cos(\alpha_n x) \right] + C \left[(S_1 + S_3) \cos(\theta_0) + (S_4 - S_2) \sin(\theta_0) \right] \quad (6)$$

θ_0 , C are constants. S_1 , S_2 , S_3 , S_4 are very rapidly convergent series which depend upon gamma function $\Gamma(z)$ and generalized Riemann's Zeta functions $\zeta(z, q)$. The latter function has been generated and tabulated using the contour expansion formulae given in [5].

Numerical Results

The boundary conditions at the metallic shielded box, plane of symmetry (ew or mw at the center $x=0$) and the dielectric interface have been checked for different field components. Fig. 1 shows the convergence behavior of $\frac{E_{x2}}{E_{y1}}$ (right below and above the interface with $\epsilon_r = 5$) as a function of n . The

figure depicts the oscillatory poor convergence of the fields at the interface ($x = 4.5 \text{ mm}$). More than 10,000 (unaccelerated series) terms is needed to get an accuracy within 10%. The worst convergence occurs along the interface as we approach the strip edges along the interface. It is important to point out that due to the rapid convergence of the series as we move away from the interface, this tremendous number of terms is only needed within a layer of thickness $\pm 0.05 \text{ mm}$ from the interface. At all other points along the different lines of force only 20 terms were used to generate the plots shown in Figs. 2,3, and 4. Fig. 2 a,b depict the dominant even mode (mw symmetry) of centered single strip at 1,15 GHz frequencies, respectively. At higher frequencies (15 GHz) the dispersion effect is apparent with more fringing field coming down from the top surface of the strip into the dielectric. Also note that the magnetic lines turn to circulate around the shielded box more in the air than in the dielectric where they try to push up towards the strip. Discontinuities of the line of force at the interface happen for a few points may lie within the poorly convergent layer. This problem is eliminated by using the accelerated series described in (6) with N of the order of 100 terms. Fig. 2c shows the odd mode (higher order) of microstrip line at $f=15 \text{ GHz}$. Figs. 4,5 show the dispersion effect at 1, 15 GHz for the dominant even and odd modes, respectively. No direct intensity comparison has been made between regions 1,2 to make the electric field lines continuous across the interface. The parameters used were $h_1 = 6 \text{ mm}$, $h_2 = 6 \text{ mm}$, $2b = 12 \text{ mm}$, $w = 1 \text{ mm}$, $w_1 = 2 \text{ mm}$, $\epsilon_r = 5$.

Conclusion

A simple method based on the transmission matrix in the fourier domain is used to generate the field plots for single and coupled strip lines at different frequencies. Even and odd modes have been generated and the dispersion effect for different modes is apparent at higher frequencies.

References

- [1] Ayman A. Mostafa, C.M. Krowne, K.A. Zaki, "Higher Order Modes of Single and Coupled Microstrips in Isotropic Dielectric Media By Spectral Matrix Method," IEEE AP-s Int. Antenna and Propagation symp. Dig., June 1987.
- [2] D. Kajfez, J. Gerald, "Plotting Vector Fields with Personal Computer," *IEEE Trans. Microwave Theory Tech.*, Vol. MTT-35, Nov. 1987.
- [3] K.A. Zaki, C. Chen, "Intensity and Distribution of Hybrid-mode Fields in Dielectric-Loaded Waveguides," *IEEE Trans. Microwave Theory Tech.*, Vol. MTT-33, pp. 1442-1447, Dec. 1985.
- [4] G.G. MacFarlane, "The Application of Mellin Transforms to the Summation of Slowly Convergent Series," *Phil Mag*, vol. 40, pp188-197, Feb. 1949
- [5] Gradshteyn, I.M. Ryzhik, *Tables of Integrals, Series and products*, Academic Press Inc. 1980.

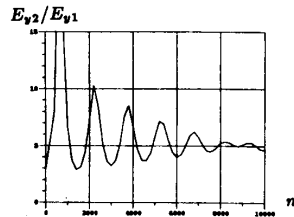


Fig. 1

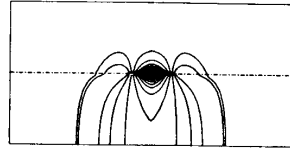


Fig. 2c Odd mode $f = 15 \text{ GHz}$.

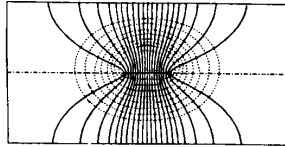


Fig. 2a Even mode $f = 1 \text{ GHz}$.

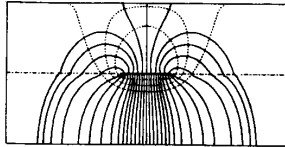


Fig. 2b Even mode $f = 15 \text{ GHz}$.

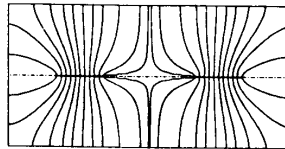


Fig. 3a $f = 1 \text{ GHz}$.

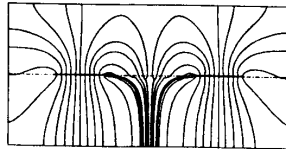


Fig. 3b $f = 15 \text{ GHz}$.

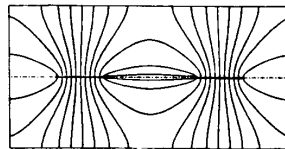


Fig. 4a $f = 1 \text{ GHz}$.

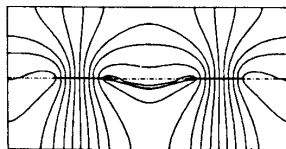


Fig. 4b $f = 15 \text{ GHz}$.

Fig. 1 Convergence of E_{y2}/E_{y1} versus n ($x = 4.5 \text{ mm}$).

Fig. 2 Field plots of single microstrip line.

Fig. 3 Coupled strip lines (even mode) $f=1,15 \text{ GHz}$.

Fig. 4 Coupled strip lines (odd mode) $f=1,15 \text{ GHz}$.